Temporal and spectral studies of high-order harmonics generated by polarization-modulated infrared fields

Sola, I. J.; Zair, A.; Lopez, Rodrigo; Johnsson, Per; Varju, Katalin; Cormier, E; Mauritsson, Johan; L'Huillier, Anne; Strelkov, V; Mevel, E.; Constant, E.

Published in:
Physical Review A (Atomic, Molecular and Optical Physics)

DOI:
10.1103/PhysRevA.74.013810

2006

Temporal and spectral studies of high-order harmonics generated by polarization-modulated infrared fields

I. J. Sola,[1,*] A. Zaïr,[1] R. López-Martens,[2] P. Johnsson,[2] K. Varjú,[2] E. Cormier,[1] J. Mauritsson,[2] A. L'Huillier,[2] V. Strelkov,[3] E. Mével,[1] and E. Constant[1]

[1]*Centre Lasers Intenses et Applications (CELIA), Domaine du Haut-Carré, Université Bordeaux 1, 351 Cours de la Libération, 33405 Talence, France*

[2]*Department of Physics, Lund Institute of Technology, P.O. Box 118, S-221 00 Lund, Sweden*

[3]*General Physics Institute of Russian Academy of Sciences, 38, Vavilova st., Moscow 119991, Russia*

(Received 8 June 2005; revised manuscript received 4 January 2006; published 21 July 2006)

The temporal confinement of high harmonic generation (HHG) via modulation of the polarization of the fundamental pulse is studied in both temporal and spectral domains. In the temporal domain, a collinear cross-correlation setup using a 40 fs IR pump for the HHG and a 9 fs IR pulse to probe the generated emission is used to measure the XUV pulse duration. The observed temporal confinement is found to be consistent with theoretical predictions. An increased confinement is observed when a 9 fs pulse is used to generate the harmonics. An important spectral broadening, including a continuum background, is also measured. Theoretical calculations show that with 10 fs driving pulses, either one or two main attosecond pulses are created depending on the value of the carrier envelope phase.

DOI: 10.1103/PhysRevA.74.013810 PACS number(s): 42.65.Ky, 42.65.Re, 32.80.Rm

I. INTRODUCTION

High harmonic generation (HHG) in gases has attracted a lot of attention over the last decade, mainly because of its potential to create attosecond pulse trains (APT) or isolated attosecond pulses. The physical process of HHG is well understood through both quantum mechanical models [1,2] and a semiclassical model [3]. According to the latter model, when an atom is irradiated by an intense laser, an electron is excited from the ground state to a continuum state, usually through tunneling ionization. Once the electron is released into the continuum, it evolves in the electric field accumulating energy. This energy can be released in the form of extreme ultraviolet (XUV) emission if the electron returns to the parent ion and recombines. The repetitive nature of this process leads to a periodic generation of XUV bursts, which in the spectral domain corresponds to odd harmonics of the fundamental frequency. It has been predicted [4,5] that the large spectral bandwidth of the harmonic emission corresponds, in time, to an APT if the harmonics are locked in phase. The individual attosecond pulses in the APT are separated by half the fundamental optical period [6].

A major challenge is to isolate a single attosecond pulse from the APT. The scheme used in the first experimental demonstration uses a spectral filter, which selects the cut-off region of a harmonic spectrum obtained from a 5 fs driving pulse [7–10]. These cut-off harmonics are only produced near the peak of the IR pulse and the emission is thus confined to half an IR cycle. Since the spectral width is limited to the cut-off region, however, the efficiency of the process is rather low and the minimum pulse duration is limited to several hundred attoseconds [11]. A scheme for the generation of isolated attosecond pulses, not limited to the cut-off region, exploits the high sensitivity of the HHG process to the IR pulse polarization; the HHG efficiency decreases rapidly with increasing ellipticity [12–14]. By varying the ellipticity of the driving pulse, with circular polarization at the wings and linear polarization at the center, the harmonic emission can be confined to shorter time scales than otherwise possible [15–18]. Different attempts based on this scheme have been reported [19–21].

For the work presented in this paper a time-gating scheme is realized that uses two $\lambda/4$ plates to obtain the required temporal variation of the polarization across the driving pulse [20]. The setup is illustrated in Fig. 1. The first $\lambda/4$ plate is of multiple order and oriented with its principal axis at an angle $\alpha=45°$ to the input IR polarization. It serves a dual purpose: (1) produce two pulses (one with ordinary and one with extraordinary polarization), and (2) introduce a time delay δ between these two pulses. The polarization of the superposed pulses after the first $\lambda/4$ plate varies from linear through circular and back to linear. The second $\lambda/4$ plate is of zero order and its principal axis is oriented at an angle β relative to the input IR polarization. This $\lambda/4$ plate changes the output polarization without changing the intensity profile. By changing β, different ellipticity variations across the output pulse can be achieved [20]. In particular, $\beta=0°$ corresponds to a case where the polarization is circular at the wings of the pulse and linear in the central region. In this configuration the temporal window where the ellipticity is sufficiently small to generate harmonics is the shortest possible and the temporal confinement is thus maximized. This configuration will therefore be referred to as the "narrow gate." For $\beta=45°$, the polarization is linear, albeit rotating by 90°, over the entire pulse and harmonics are generated over a longer time. This configuration is referred to as the "large gate." For $\alpha=\beta=0°$, we retrieve the unaltered incident IR pulse with a linear polarization at a constant direction. This configuration is referred to as the "no gate." The technique used to achieve the time gating is experimentally interesting

*Present address: Departamento de Física Aplicada, University of Salamanca, Pl. de la Merced s/n, 37008 Salamanca, Spain.

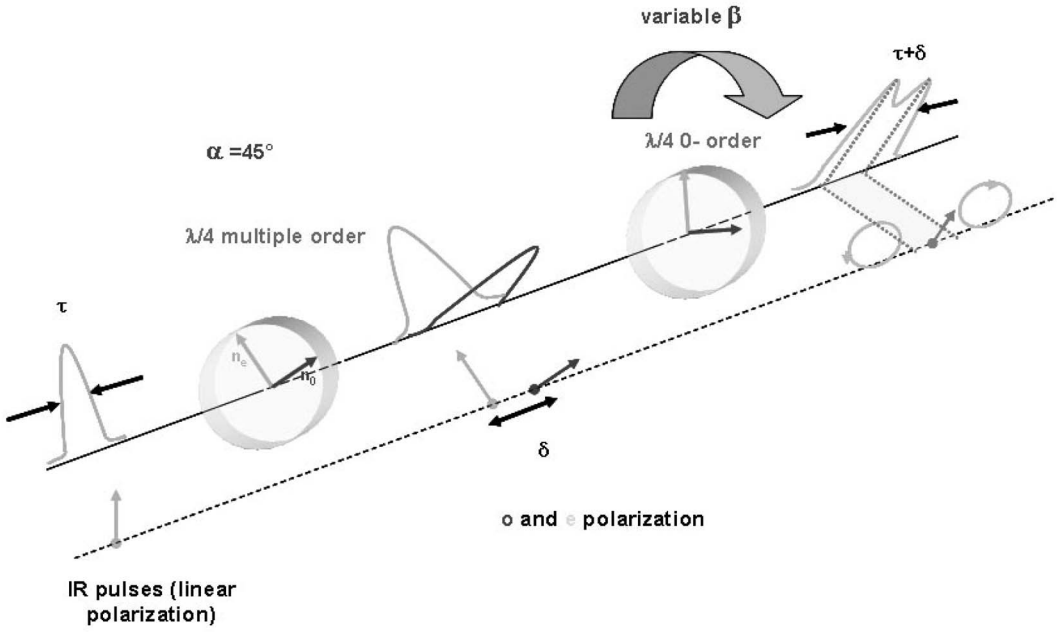

FIG. 1. Polarization gate setup. The linear polarized pulse (duration τ) passes through a multiple order quarter-wave plate, whose axes form an angle $\alpha=45°$ related to the incident polarization direction. The plate introduces a delay δ between the ordinary and extraordinary components. The output pulse presents a polarization modulation from linear in the pulse wings to circular in the center. A zero order quarter-wave plate, whose axes form an angle β, changes this ellipticity evolution. If $\beta=0°$ (narrow gate), circular polarization is turned into linear and vice versa.

because it is robust, simple and provides the possibility to control, in a continuous fashion via the angle β, the duration of the ellipticity gate.

In the first works [20], the effect of the polarization modulation was observed in the spectral domain, using pulses with durations down to 30 fs. However, spectral measurements provide only indirect information about the temporal structure of the XUV pulses, lacking information about the spectral phase. The first measurement of the time structure of the temporally confined harmonic emission [22,23] used a cross-correlation technique [24]. This experiment showed that gating the ellipticity results in a temporal confinement of the harmonic emission. Nevertheless, the use of noncollinear pump-probe geometry limited the temporal resolution of this measurement to 15–20 fs and the maximum observed confinement was therefore limited by the experimental resolution. In the present work we use a collinear pump-probe geometry, which results in an improved temporal resolution (around 9 fs) and we present both temporal and spectral measurements. The temporal measurements, described in Sec. II, are performed using 40 fs pulses to generate the harmonics and the results agree very well with the theoretical predictions. In Sec. III, we present spectral measurements using very short IR pulses ($\tau<10$ fs) to drive the harmonic generation. In these conditions we observe a spectral broadening towards a continuum, consistent with the emission of a single attosecond pulse. Theoretical simulations have been performed in order to understand this effect. In Sec. IV, the results are discussed together with future perspectives.

II. TEMPORAL MEASUREMENTS

Temporally resolved measurements of the harmonic emission are of special interest, since they give direct information about the temporal confinement achieved using the ellipticity gate technique. In the cross-correlation technique used in the present work [24], the generated harmonic pulses are overlapped, spatially and temporally, with an IR probe pulse and the total electromagnetic field ionizes an atomic gas inside a magnetic bottle electron spectrometer (MBES). The cross-correlation signals are the sidebands to the principal peaks (due to the harmonics only) in the photoelectron spectrum. The time structure of the harmonic emission can be determined by varying the delay between the two pulses and by recording the variation of the sideband peaks, since their amplitude depends on the temporal overlap of the XUV and IR pulses [25,26]. The resolution of this technique is given by the IR pulse duration and the geometrical configuration. In the present work, the collinear overlap of the IR probe and the XUV pump leads to a 9 fs resolution, only limited by the probe duration.

In Fig. 2, we present the experimental setup used to perform the cross-correlation measurements. The input IR pulses ($E=2$ mJ, $\tau=40$ fs) are divided in two using a 50/50 beam splitter. The reflected beam, which is used to generate the harmonics, passes through the two $\lambda/4$ plates that form the time-gate system and is focused by a spherical mirror ($f=50$ cm) into a 2-mm-wide Xe gas cell. A 0.2 μm Al filter is positioned after the generation and used to remove the fundamental IR radiation. This filter also removes the low harmonic orders, up to the 11th harmonic. The 1 mJ probe pulse that is transmitted through the beam splitter is post-compressed using the hollow waveguide technique [27,28]. The beam is coupled into a hollow waveguide filled with Ar at a pressure of 300 mbar. After the waveguide, the pulse, which is spectrally broadened through self-phase modulation

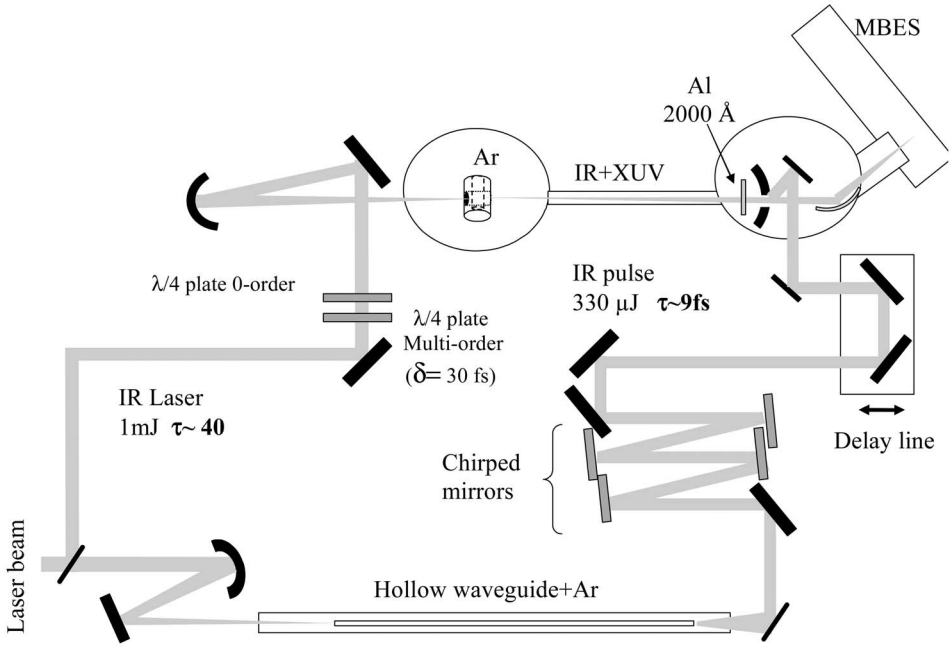

FIG. 2. Cross-correlation experimental setup.

in the gas, is compressed by negatively chirped mirrors. The compressed pulse has 9 fs duration and 300 μJ energy. A spectral interferometry for direct electric field reconstruction (SPIDER) system [29] is used to characterize both the pump and the probe IR pulses. The XUV pump and the IR probe pulses are recombined using a convex mirror with a hole in the center. The XUV pump passes through this hole while the IR probe is reflected by the mirror. The curvature of the mirror is chosen such that the two beams, from this point, have the same divergence. Finally, both beams are focused into the MBES filled with a static pressure of argon gas.

The multiorder $\lambda/4$ wave plate has a thickness of 1.01 mm, resulting in a delay $\delta=30$ fs between the ordinary and extraordinary polarization components. Figure 3 shows the photoelectron spectra for different delays between the IR and the XUV pulses. The harmonic signal is present for every delay, but only when there is a temporal overlap of both pump and probe, can two color photon phenomena happen. Then the photoelectrons released from a XUV photon absorption and the emission or absorption of an IR photon yield to the presence of sidebands between the harmonic peaks. Knowing the IR pulse and the evolution of the sideband signals depending on the pump-probe delay, one can extract the XUV pulse train duration by deconvolution. One can then study the XUV pulse train duration as a function of the polarization gate width.

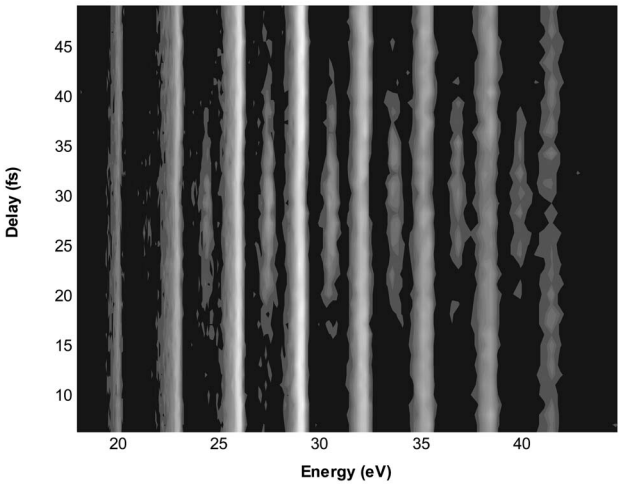

FIG. 3. MBES spectra depending on probe delay. No gate configuration.

Having fixed the angle α of the first quarter-wave plate at 45°, the angle β of the second one is changed, which alters the gate configuration from large gate ($\beta=(2n+1)\pi/4$ rad, n is an integer) to narrow gate ($\beta=n\pi/2$) [20]. Figure 4(a) shows the temporal structure of the 18th sideband (between the 17th and 19th harmonics) for the three configurations: large, narrow, and no gate. Comparing with the "no gate" case, the width of the sideband is decreased in the narrow gate configuration and increased when the large gate is used. Figure 4(b) shows the harmonic pulse widths, obtained using the procedure described in Ref. [22], for large, narrow, and no gate. For the large gate situation a correction has been included to take into account the evolution of the detector response with the polarization orientation (as presented in Ref. [22]). In the same figure we present the narrow gate width calculated using the analytical expression (3) from Ref. [30] equal to 11.5 fs for the present experimental conditions. According to this expression, the gate width τ_g in the narrow gate configuration is given by $\tau_g=\varepsilon_{\text{thr}}\tau^2/[\ln(2)\delta]$, where δ is, as previously commented, the delay induced by the first quarter-wave plate between the ordinary and extraordinary components, τ the minimum pulse duration, and ε_{thr} the threshold ellipticity, defined as the field ellipticity for which the harmonic signal is decreased to 50% of the maximum signal (obtained for $\varepsilon=0$). One can see that the experimental results agree very well with this theoretical prediction. Note that the confinement is identical for four plateau

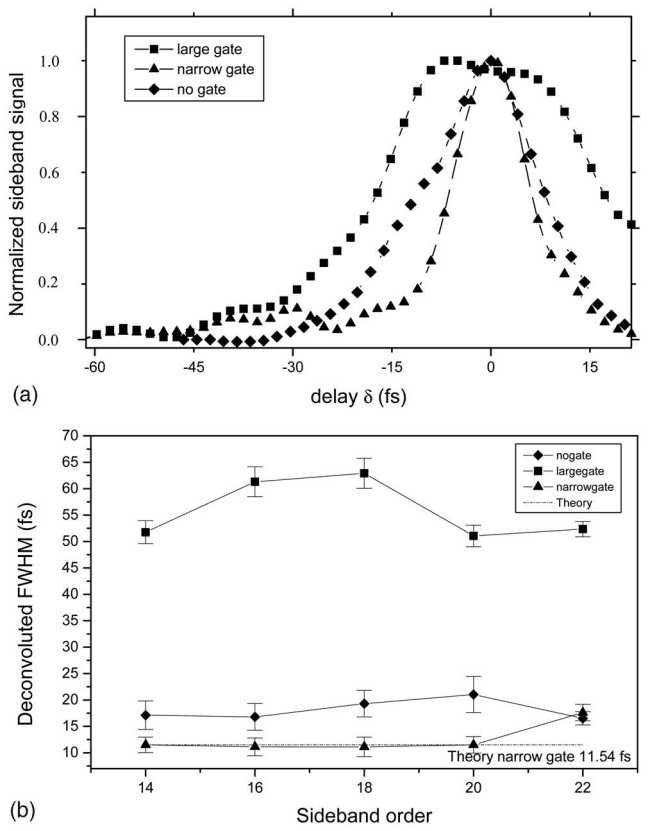

FIG. 4. (a) Evolution of the intensity of the 18th sideband as a function of the pump-probe delay for several gate configurations: narrow gate (triangles), large gate (squares), and no gate (diamonds). (b) Deconvolution of the sideband widths (FWHM) by the IR pulse, corresponding to narrow gate (triangles), large gate (squares), and no gate (diamonds) configurations for the different sidebands.

sidebands (14–20). The discrepancy observed for the 22nd sideband is not relevant since the low sideband signal results in large uncertainty. In general, our results are fully consistent with the recently reported measurement using the XUV SPIDER technique for a single harmonic [31]. This technique is a promising future alternative when applied to the different harmonics, since, considering Ref. [31], experimental precision can be estimated on 1 fs. Nevertheless, in our case the cross-correlation resolution, depending on the probe duration (9 fs) allows us to observe the temporal confinement effect and check the analytical expression accuracy in ultrashort conditions.

In conclusion, these measurements show that the ellipticity gating technique results in a temporal confinement of the harmonic emission, in good quantitative agreement with theory. Between the narrow and the no gate case, the pulse train duration is reduced by a factor of 1.5–1.7 even using this limited gating configuration.

III. SPECTRAL MEASUREMENTS

In order to study the effect of the time gate technique on harmonics generated by very short IR pulses, the setup in

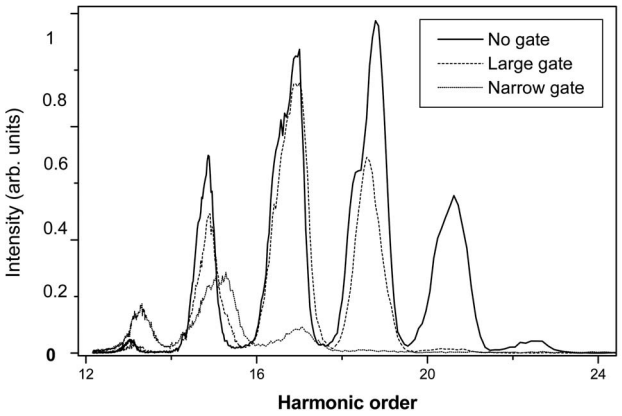

FIG. 5. Harmonic spectra corresponding to narrow (dotted), large (dashed-dotted), and no gate (solid) configurations, for the experimental conditions $\tau=9$ fs, $\delta=10$ fs.

Fig. 2 was modified so that the compressed pulse ($\tau=9$ fs and $E=300$ μJ) was used to drive the harmonic generation after having passed through two quarter-wave plates. The dispersion of the $\lambda/4$ plates and of the entrance window to the vacuum chamber was precompensated for, so that the pulse was transform limited when it reached the generation gas. The multiorder $\lambda/4$ plate (314 μm width) used introduced a delay $\delta=10$ fs between the ordinary and extraordinary polarization, resulting in a flat top intensity profile and a narrow gate whose duration is 1.75 fs according to the analytical expression. No time domain measurements were performed with this pulse configuration due to the limited temporal resolution of our cross-correlation setup. The measurements were instead done in the spectral domain, from harmonics 13 to 23.

Figure 5 shows three normalized spectra corresponding to the narrow, large, and no gate configurations. The spectral width of the harmonics is obviously narrower in the no gate and large gate cases. The no gate result exhibits a larger number of harmonics, simply because the peak intensity is higher. In the narrow gate case, the harmonic spectral width is much larger (about twice as large), and the intensity does not fall to zero between the peaks.

To investigate the spectral dependence on the gate width, the angle β was varied (while keeping $\alpha=45°$) and the spectral width (FWHM) of harmonics 15 and 17 were measured and plotted in Fig. 6. The narrowest spectra (0.8 eV) corresponds, as expected, to the large gate configuration, while the narrow gate spectrum is the broadest, consistent with the temporal confinement. In the narrow gate configuration both harmonics 15 and 17 have a FWHM of 1.8 eV, which corresponds roughly to half the spectral gap between two consecutive harmonic peaks. Assuming, as a simplifying hypothesis, that the harmonics are near transform-limited and locked in phase, this corresponds to a train consisting of only two attosecond pulses. This result agrees well with the theoretical width of the time gate, 1.75 fs, corresponding to the emission of two pulses.

The ultimate goal with this technique is to confine the XUV emission to a single attosecond pulse, which requires the creation of a gate shorter than a half optical cycle. There

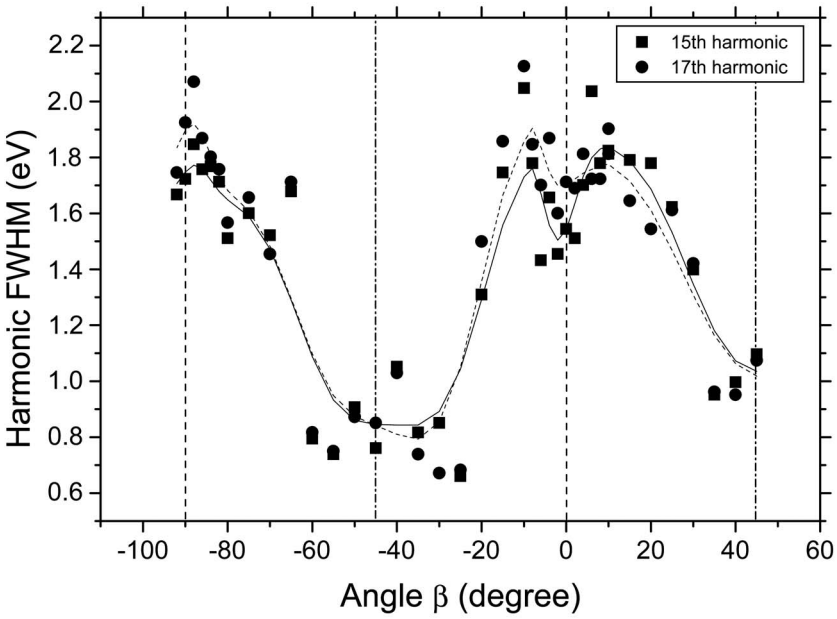

FIG. 6. 15th and 17th harmonic spectral FWHM depending on angle β (τ=9 fs, δ=10 fs).

are two experimental approaches to produce a gate that is sufficiently narrow to obtain this goal: (1) using shorter IR pulses; or (2) a larger delay δ. In the current experiment, the first approach was not possible. The second approach could be implemented simply by using a thicker multiorder $\lambda/4$ plate. The main drawback of this approach is that the intensity profile is no longer a flat top, but presents a dip at the center (when $\delta > \tau$). This significantly reduces the harmonic generation efficiency in the narrow gate configuration since the temporal window where the harmonics are generated (i.e., where the ellipticity is small) coincides with a local minimum in the intensity profile.

Therefore, for this measurement a multiorder $\lambda/4$-plate is used (470 μm width) introducing a 15 fs delay and obtaining a narrow gate very close to the half optical cycle (according to the analytical expression the gate width is equal to 1.2 fs) while creating an important intensity dip in the central region of the pulse (30–40% of the maximum intensity of the ellipticity-modulated pulse). The harmonics were generated by focusing 9 fs 350 μJ IR pulses into a 15-mm-long cell filled with Ar at a pressure of 30 mbar low enough to avoid a dramatic effect of the medium ionization on the laser pulse propagation. To increase the spectral resolution and sensitivity, a photon spectrometer with a photomultiplier was used instead of the MBES.

In Fig. 7(a), we show the harmonic spectrum (averaged over several shots) for the no gate configuration ($\alpha=\beta=0°$). The absence of low harmonics (below 35 eV) is likely due to the high absorption in the HHG cell, which acts as a spectral filter. Simulations with the experimental gas pressure and the focal point inside the cell show, indeed, very low transmission below 35 eV. In the narrow gate configuration [Fig. 7(b)], the spectrum is broadened and becomes almost a continuum, in agreement with the results on Ref. [21]. Some harmonic structures remain, however, resembling those obtained with τ=9 fs, δ=10 fs. As we have yet mentioned, in the narrow gate configuration for τ=9 fs, δ =15 fs the gate width is very close to half an optical period. In this case, depending on the carrier envelope phase (CEP) either a single attosecond pulse with a spectral continuum, or two pulses with the broad harmonic structures (as seen before) can be generated [30,32–34]. Since the obtained results are averaged over several shots and the CEP is not stabilized, the observed spectrum should be a superposition of spectra corresponding to the emission of either one or two attosec-

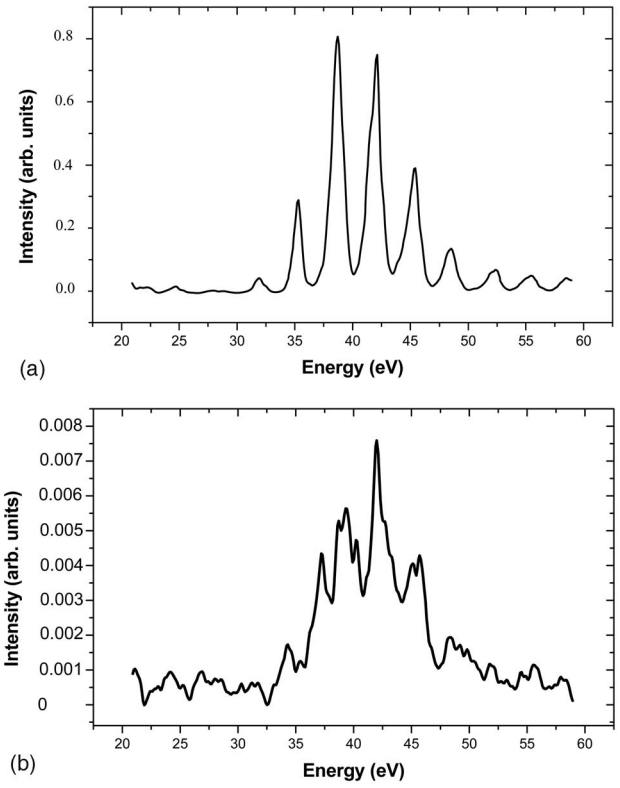

FIG. 7. (a) XUV spectrum in the no gate configuration (τ=9 fs). (b) XUV spectrum in the narrow gate configuration (τ=9 fs, δ=15 fs).

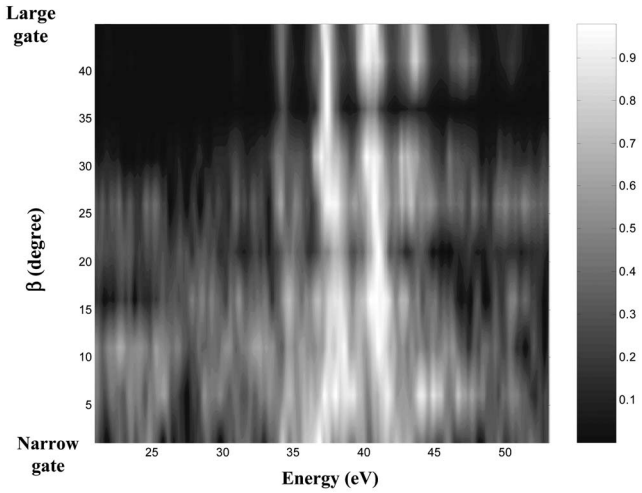

FIG. 8. Normalized XUVspectrum evolution depending on angle β (τ=9 fs, δ=15 fs).

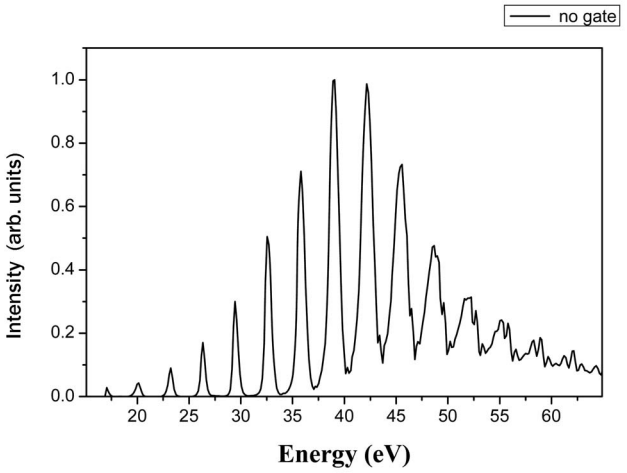

FIG. 9. XUV spectrum simulated in the no gate configuration (τ=10 fs) averaged over different IR pulse CEP values.

ond pulses. The observed spectra are consistent with this analysis.

The influence of the IR pulse duration on the harmonic spectrum has also been investigated by changing the post-compression so that the pulse duration increases from 9 to 10.5 fs. The harmonic spectrum is then changed from the quasicontinuum shown in Fig. 7(b) to well resolved harmonic structures as seen in the δ=10 fs experiment (see Fig. 4). When τ is slightly increased, the time gate becomes larger, and the generation of two pulses is more frequent than that of a single one. The harmonic peaks in the spectrum, therefore, become more pronounced. The transition is abrupt and consistent with the theoretically predicted half period time gate.

In Fig. 8 the normalized spectra are shown as a function of the angle β of the second $\lambda/4$-plate (for δ=15 fs and τ=9 fs). The figure shows a clear change from narrow harmonic structures in the large gate configuration (β=45°) to broad features for the narrow gate, consistent with a continuous change in the confinement of the XUV emission. This change occurs in a relatively narrow range of values of angles β, as mentioned in Ref. [22]. The spectral change is obtained simply by rotating a plate, showing the simplicity and robustness of the method.

As was shown in Sec. II, using the 40 fs long incident laser pulse we generate the XUV train with the duration that agrees very well with the analytical formula from Ref. [30]. However, in the case of 10 fs driving laser pulses considered in the present section, this approximate formula overestimates slightly [30,34] the attopulses train duration. To study more accurately the temporal structure of the attopulse train in this case we calculate the XUV generation utilizing the theoretical approach that we developed and used in our previous papers [30,33,34].

Our theory for the single-atom response is intermediate between the analytical approaches [1,2] and the numerical solution of the time-dependent Schrödinger equation. This theory was suggested [35] for the linearly polarized driving field and further developed for the arbitrary fundamental polarization [33]. The approach is based on the three-step model for the HHG [3]. Our theory includes the numerically calculated ionization rate and considers the electron wave-packet spreading after the ionization using the results of Ref. [36]. For the middle-plateau harmonics, there are several significantly different electron quantum paths [1,2] that lead to the generation of the radiation with the same frequency, albeit different phase properties. In our theory the contributions of these quantum paths are separated yet within the frame of the single-atom response. Due to the numerically calculated ionization rate and the accurate consideration of the wave-packet spreading our theory provides the correct ratio of the impacts of the different quantum paths in the XUV generation. Moreover, in our theory the ground state population at the instant of the ionization and the instant of the XUV emission are calculated separately, in contrast with theories [1,2] that suppose adiabatic variation of the ground state population and thus do not distinguish the population difference in these instants. However, if the laser intensity is high the ionization is not adiabatic any more and these populations should be considered separately as it was recently confirmed with numerical results [37]. Using this theory for the single-atom response, we calculate the medium response taking into account the phase-matching effects for the XUV generation, as well as its reabsorption by the generating gas; our approach for the medium response calculation is described in Ref. [33,38].

In Fig. 9 we present the XUV spectrum simulated considering 10 fs IR pulses in the no gate configuration. In the calculation we set Ar pressure as 40 mBar and peak laser intensity as 1.6×10^{15} W/cm^2. The latter value is found from the measured energy of the IR pulse and focusing conditions. The geometrical parameters in the calculation also reproduce experimental ones. The spectrum is averaged over the CEP values of the IR pulse. The averaging is used in this figure as well as in the next one to mimic the experiment which is not CEP stabilized. However, in this situation no relevant CEP dependence has been observed, since it is a multicycle regime. The main features observed experimentally in Fig. 7(a) are reproduced by the simulation.

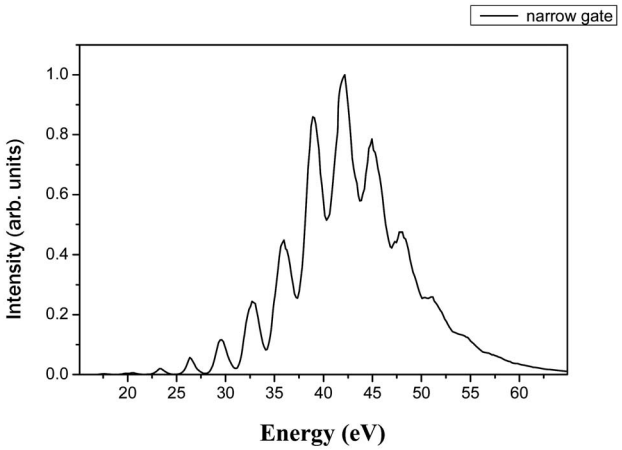

FIG. 10. XUV spectrum simulated in the narrow gate configuration (τ=10 fs, δ=15 fs) averaged over different IR pulse CEP values.

Figure 10 shows the XUV spectrum calculated in the narrow gate (τ=10 fs, δ=15 fs) configuration, averaged over several IR pulse CEPs. Other parameters are the same as in the previous figure (note that the same incident laser pulse now provides the peak intensity in the center of the gate equal to 3.3×10^{14} W/cm^2). In these conditions, the spectra dependence on the CEP value is very pronounced (in contrast with the no gate configuration). Therefore, although spectra for a given CEP usually contains well-distinct harmonic structure, averaging of the spectrum over the CEPs yields a quasicontinuous spectrum with some narrow peaks.

Agreement between an experimental spectrum [Fig. 7(b)] and a simulated one (Fig. 10) is very good, even quantitatively, presenting the same structure. The agreement confirms the reliability of our calculation. This is very important because the calculation provides results both in spectral and temporal domain, while in our experiments subfemtosecond temporal measurements were not available. In fact, Fig. 11 shows the attosecond pulses calculated at the beam axis for conditions of Fig. 10 corresponding to different CEPs of the IR pulse. The total radiation with photon energy higher than the Ar ionization energy is used to obtain the attopulses. Here the CEP dependence is evident, as for some situation (CEP=π/2) a main attosecond burst with two small satellites is obtained, and for other (CEP=0) two clear pulses are generated. The CEP value ϕ is defined here as in Ref. [33].

One can assume that a rapid temporal variation of the ellipticity might affect the duration of an individual attopulse. To study this item we compare the duration of the attopulses simulated with and without the polarization gating technique. The confined train attopulses presented in Fig. 11 have durations of 160–200 as depending on the CEP, while the attopulses calculated for the no gate configuration (for the conditions of Fig. 9) have durations of 130–180 as depending on the attopulse position in the train. Thus, according to simulations, the pulses in the confined train are comparable in duration to ones in the nonconfined train. Therefore, we show that the polarization-gating technique does not introduce an important individual attopulse broadening. This result is in clear agreement with a recently published work [39].

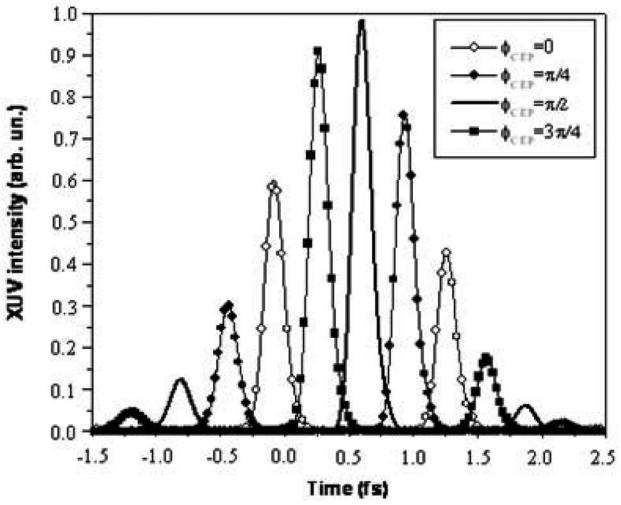

FIG. 11. XUV attopulses simulated in the narrow gate configuration (τ=10 fs, δ=15 fs) for different IR pulse CEPs (0, π/4, π/2, and 3π/4).

IV. CONCLUSIONS

Using a collinear IR-XUV cross-correlation setup we have directly measured the temporal confinement of the XUV emission from HHG using the time-gating technique. This experiment complements and improves a previous one [20], showing the effect with a better temporal resolution. The experimental results agree well with the theoretical description.

When short (9 fs) IR pulses are used to generate harmonics with the time-gate technique, near continuum XUV spectra are obtained, compatible with the emission of one or two attosecond pulses. Theoretical simulations have been developed, presenting good agreement with the experiment. They predict that the duration of the attosecond pulses is approximately the same as one of the pulses emitted without a time gate.

The presented approach for XUV generation temporal gating is simple and robust and allows a continuous control of the temporal confinement over a broad spectral range.

When the HHG is confined to half an IR optical cycle, the CEP becomes an important parameter for the number of generated attosecond pulses. In the presented experiment, the CEP is random and either one or two pulses can be emitted. However, if the CEP is stabilized and set to a proper value, single attosecond pulses can be produced for each laser pulse. As a future perspective, the combining of the time-gating technique with CEP stabilization will provide a stable source of single attosecond pulses from 9 fs IR pulses. If the CEP stabilization is not available, shorter IR pulses, of the order of 6 fs and/or longer delays can be used. In these conditions, CEP fluctuations would lead to either no XUV emission or a single as pulse emission.

ACKNOWLEDGMENTS

This work has been supported by the Research Training Network ATTO (Grant No. HPRN-2000-00133), a Marie Curie Intra-European Foundation (Grant No. MEIF-CT-2004-009268), the Marie Curie Research Training Network XTRA (Grant No. MRTN-CT-2003-505138), the Integrated Initiative of Infrastructure LASERLAB-EUROPE (Grant No. RII3-CT-2003-506350), the Knut and Alice Wallenberg Foundation, the Swedish Science Council, the funding from the Région Aquitaine ("Allocation de Recherche de la Région Aquitaine, project Physique Attoseconde et Application, convention 20040205001A"), the Russian Academy of Science (Program "Femtosecond optics and superintense laser fields physics"), and the European Regional Development Funds (FEDER). We acknowledge technical support by D. Descamps and S. Petit.

[1] M. Lewenstein, P. Balcou, M. Y. Ivanov, A. L'Huillier, and P. B. Corkum, Phys. Rev. A **49**, 2117 (1994).
[2] W. Becker, S. Long, and J. K. McIver, Phys. Rev. A **50**, 1540 (1995).
[3] P. B. Corkum, Phys. Rev. Lett. **71**, 1994 (1993).
[4] G. Farkas and C. Toth, Phys. Lett. A **168**, 447 (1992).
[5] S. E. Harris, J. J. Macklin, and T. W. Hänsch, Opt. Commun. **100**, 487 (1993).
[6] P. M. Paul *et al.*, Science **292**, 902 (2001).
[7] M. Protopapas, D. G. Lappas, C. H. Keitel, and P. L. Knight, Phys. Rev. A **53**, R2933 (1996).
[8] Ch. Spielmann, N. H. Burnett, S. Sartania, R. Koppistch, M. Schnürer, C. Kan, M. Lenzer, P. Wobrauschek, and F. Krausz, Science **278**, 661 (1997).
[9] K. J. Schafer and K. C. Kulander, Phys. Rev. Lett. **78**, 638 (1997).
[10] I. P. Christov, M. M. Murnane, and H. C. Kapteyn, Phys. Rev. Lett. **78**, 1251 (1997).
[11] M. Hentschel, R. Kienberger, Ch. Spielmann, G. A. Reider, N. Milosevic, T. Brabec, P. Corkum, V. Heinzmann, M. Drescher, and F. Kausz, Nature (London) **414**, 509 (2001).
[12] K. S. Budil, P. Salières, A. L'Huillier, T. Ditmire, and M. D. Perry, Phys. Rev. A **48**, R3437 (1993).
[13] Y. Liang, M. V. Ammosov, and S. L. Chin, J. Phys. B **27**, 1296 (1994).
[14] P. Dietrich, N. H. Burnett, M. Y. Ivanov, and P. B. Corkum, Phys. Rev. A **50**, R3585 (1994).
[15] P. B. Corkum, N. H. Burnett, and M. Y. Ivanov, Opt. Lett. **19**, 1870 (1994).
[16] V. T. Platonenko and V. V. Strelkov, J. Opt. Soc. Am. B **16**, 435 (1999).
[17] P. B. Corkum, Opt. Lett. **19**, 22 (1994).
[18] Z. Chang, Phys. Rev. A **70**, 043802 (2004).
[19] C. Altucci, C. Delfin, L. Roos, M. B. Gaarde, A. L'Huillier, I. Mercer, T. Starczewski, and C.-G. Wahlström, Phys. Rev. A **58**, 3934 (1998).
[20] O. Tcherbakoff, E. Mével, D. Descamps, J. Plumridge, and E. Constant, Phys. Rev. A **68**, 043804 (2003); E. Constant, Ph.D. thesis 1997 (unpublished).
[21] B. Shan, S. Ghimire, and Z. Chang, J. Mod. Opt. **52**(2-3), 277 (2005).
[22] R. López-Martens, J. Mauritsson, P. Johnsson, A. L'Huillier, O. Tcherbakoff, A. Zaïr, E. Mével, and E. Constant, Phys. Rev. A **69**, 053811 (2004).
[23] A. Zaïr, O. Tcherbakoff, E. Mével, E. Constant, R. López-Martens, J. Mauritsson, P. Johnsson, and A. L'Huillier, Appl. Phys. B: Lasers Opt. **78**, 869 (2004).
[24] J. Mauritsson, P. Johnsson, R. López-Martens, K. Varjú, W. Kornelis, J. Biegert, U. Keller, M. B. Gaarde, K. J. Schafer, and A. L'Huillier, Phys. Rev. A **70**, R021801 (2004).
[25] T. E. Glover, R. W. Schoenlein, A. H. Chin, and C. V. Shank, Phys. Rev. Lett. **76**, 2468 (1996).
[26] A. Bouhal, P. Salières, P. Breger, P. Agostini, G. Hamoniaux, A. Mysyrowicz, A. Antonetti, R. Constantinescu, and H. G. Muller, Phys. Rev. A **58**, 389 (1998).
[27] M. Nisoli, S. De Silvestri, and O. Svelto, Appl. Phys. Lett. **68**, 2793 (1996).
[28] M. Nisoli, S. De Silvestri, O. Svelto, R. Szipöcs, K. Ferencz, C. Spielmann, S. Sartania, and F. Krausz, Opt. Lett. **22**, 522 (1997).
[29] C. Iaconis and I. A. Walsmey, Opt. Lett. **23**, 792 (1998).
[30] V. Strelkov, A. Zair, O. Tcherbakoff, R. Lopez-Martens, E. Cormier, E. Mével, and E. Constant, J. Phys. B **38**, L161 (2005).
[31] Y. Mairesse, O. Gobert, P. Breger, H. Merdji, P. Meynadier, P. Monchicourt, M. Perdrix, P. Salières, and B. Carré, Phys. Rev. Lett. **94**, 173903 (2005).
[32] A. Baltuska, Th. Udem, M. Uiberacker, M. Hentschel, E. Goulielmakis, Ch. Gohle, R. Holzwarth, V. S. Yakovlev, A. Scrinzi, T. W. Hänsch, and F. Krausz, Nature (London) **421**, 611 (2003).
[33] V. Strelkov, A. Zaïr, O. Tcherbakoff, R. López-Martens, E. Cormier, E. Mével, and E. Constant, Appl. Phys. B: Lasers Opt. **78**, 879 (2004).
[34] V. Strelkov, A. Zair, O. Tcherbakoff, R. Lopez-Martens, E. Cormier, E. Mével, and E. Constant, Laser Phys. **15**, 871 (2005).
[35] V. T. Platonenko, Quantum Electron. **31**, 55 (2001).
[36] A. M. Perelomov, V. S. Popov, and M. V. Terent'ev, JETP Lett. **50**, 1393 (1966) [Sov. Phys. JETP **23**, 924 (1966)].
[37] V. V. Strelkov, A. F. Sterjantov, N. Yu. Shubin, and V. T. Platonenko, J. Phys. B (to be published).
[38] V. T. Platonenko, V. Strelkov, and G. Ferrante, J. Opt. Soc. Am. B **19**, 1611 (2002).
[39] Z. Chang, Phys. Rev. A **71**, 023813 (2005).